Draft version June 18, 2018
Preprint typeset using LaTeX style AASTeX6 v. 1.0

EVOLUTION OF CIRCUMBINARY PROTOPLANETARY DISKS WITH PHOTOEVAPORATIVE WINDS DUE TO EXTERNAL FAR ULTRAVIOLET RADIATION

M. Shadmehri, S. M. Ghoreyshi*, N. Alipoor*
Department of Physics, Faculty of Science, Golestan University, Gorgan 49138-15739, Iran

ABSTRACT

Lifetime of the protoplanetary disks (PPDs) are beleived to be severely constrained by material depleting mechanisms, including photoevaporative winds due to the internal or external radiation sources. Most previous studies focused on exploring role of the winds in the exposed PPD with a single star, however, exploring evolution of the circumbinary disks with phtoevaporative winds due to external radiation sources deserve further investigation. In this study, we follow evolution of circumbinary PPDs with photoevaporative winds due to the external FUV radiation field. We show that this mass losing process severely constrain a PPD properties, including its lifetime, mass and radius. Lifetime of a circumbinary PPD, for instance, is found to be a factor of [about 2] longer than a circumstellar analogue. [We find that this value strongly depends on the viscosity parameter.] **To be completed ...**

Keywords: accretion – accretion disks – planetary systems: protoplanetary disks

1. INTRODUCTION

Since the planet formation time-scale should not exceed lifetime of the protoplanetary disks (PPDs), constraining their lifetime plays an essential role in the current theories of planet formation (for recent reviews, e.g., Armitage 2011; Ercolano & Pascucci 2017). Magnetically-driven winds (Blandford & Payne 1982) or photoevaporative mechanisms (e.g., Alexander et al. 2006; Gorti et al. 2009) and mass accretion onto the central star or already formed planets are efficient mass depletion processes that will eventually lead to a PPD dispersal. The relative importance of these mass-loss processes, however, strongly depends upon a PPD physical properties. While magnetized winds are known to be effective at the inner region of a PPD, photoevaporation due to the radiation field of the central star (e.g., Alexander et al. 2006; Gorti et al. 2009) or its ambient stars are efficient at the outer part (Anderson et al. 2013). Current theoretical models suggest that PPDs lifetime is less than ??. Furthermore, properties of the molecular cloud cores within which PPDs are thought to be formed can dramatically impact PPDs lifetime. (Li & Xiao 2016; Xiao & Chang 2018).

The mass-loss rate due to the radiation field from the central star or external sources, as evaporative agents in the disc erosion, is a key parameter in the disc models with the photoevaporative winds. Primary focus of most previous studies was to elaborate role of the internal sources, including X-ray (e.g., Owen et al. 2010, 2011) and UV-radiation (e.g., Alexander et al. 2006), in the dispersal of PPDs where are in the isolated areas. But PPDs residing in populated regions that contain OB stars are exposed to their ambient radiation field too. Anderson et al. (2013) (hereafter; AAN2013) studied evolution of a viscous disc with photoevaporation due to FUV radiation flux from external stars using existing photoevaporative models. In order to explore the relative importance of the internal and externals radiation fields in the disc erosion, they also considered X-ray photoevaporation due to the host stars and found that external sources are dominant in the dispersal of a PPD with a solar-mass host star. A PPD lifetime, its mass and radius, therefore, are constrained severely due to the external FUV radiation field (AAN2013).

Following recent discoveries of the circumbinary planets (Doyle et al. 2011; Orosz et al. 2012; Schwamb et al. 2013), there is a growing interest for studying evolution of a PPD with a binary system at its center. Theoretical attempts to model circumbinary discs, however, started decades before recent discovery of the circumbinary discs mostly motivated by ?. Following lines of the standard disc model Shakura & Sunyaev (1973) with incorporating the binary torque, various circumbinary disc models have been developed over recent years (e.g., Martin et al. 2013). Numerical models ??. Rosotti & Clarke (2018) studied evolution of the discs around components of a binary system with photoevaporation by X-rays from

m.shadmehri@gu.ac.ir (MS)
*Iran Science Elites Federation postdoctoral fellow

the respective star.

Vartanyan et al. (2016) developed a circumbinary disk model without winds to explore steady-state structure of the disc analytically and its evolution via numerical methods. Their analysis showed that binary torque at the inner edge has a profound effect on the disc structure at all radii. They showed a circumbinary disc evolves with a significantly reduced accretion rate at its inner edge in comparison to a similar disk with a single star. A circumbinary disk, therefore, evolves on a longer timescale in comparison to a cicumstellar disk counterpart.

In the light of this finding and prominent role of photoevaporative winds in shortening a disk lifetime, it is worthwhile exploring structure of a circumbinary disk in the presence of this mass-losing process. This problem has been addressed by Alexander (2012) who studied evolution of a circumbinary disk with photoevaporative winds due to the radiation field of the host stars. Although he found that a circumbinary disk evolves with a larger surface density comparing to a disc counterpart with single star, he did not quantified disk lifetime, its mass and radius. Alexander (2012) primarily studied role of the internal radial field in a circumbinary disk erosion, whereas we plan to investigate constraints on a circumbinary PPD quantities due to the external radiation field which is a dominant evaporative source in the disks with a solar-mass host star according to AAN2013. We, therefore,

2. BASIC EQUATIONS

A circumbinary PPD is modeled as a thin disc with a binary system at its center. Orbital plane of the binary with the primary and the secondary masses $M_{\rm p}$ and $M_{\rm s}$, [and semimajor axis $a_{\rm b}$] is assumed to be coplanar with the disc. [Note that the mass ratio of its components $q \equiv Ms/Mp$ is a number less than or equal to unity.] Although the disc is subject to a time varying gravitational potential due to the binary orbital motion, as an approximation, we assume that the disc is rotating in the potential arising from the total mass, i.e., $M_{\rm c} = M_{\rm p}+M_{\rm s}$. Disc rotation profile, therefore, is Keplerian with the angular velocity $\Omega = (GM_{\rm c}/r^3)^{1/2}$. All disc quantities, furthermore, are assumed to be dependent only on the radial distance r.

Under theses circumstance and following the standard approach for constructing a thin disc model (Shakura & Sunyaev 1973), the surface density evolution equation for a circumbinary disc in the presence of the wind mass-loss is

$$\frac{\partial \Sigma}{\partial t} = \frac{1}{r}\frac{\partial}{\partial r}\left[3r^{1/2}\frac{\partial}{\partial r}\left(\nu\Sigma r^{1/2}\right) - \frac{2\Lambda\Sigma}{\Omega}\right] - \dot{\Sigma}_{\rm w}. \quad (1)$$

where ν is the turbulent viscosity and Λ is the specific angular momentum injection rate by the binary. Rate of the wind mass-loss is denoted by $\dot{\Sigma}_{\rm w}$. If the angular momentum injection rate set to be zero and wind mass-loss is neglected, the above equations reduces to the surface density evolution equation for a disc surrounding a single star. In the presence of the wind, i.e. $\dot{\Sigma}_{\rm w} \neq 0$, the equations describes a disc with wind mass-loss around a single star. Our focus, instead, is exploring evolution of a circumbinary disc with wind mass-loss. In doing so, we have to specify three important quantities.

The first key quantity is the turbulent viscosity ν [$(= \alpha c_s^2/\Omega)$, where $c_s = \sqrt{k_{\rm B}T/\mu}$ is sound speed]. Disc turbulence is thought to be driven by the fluid instabilities, including magnetorotational instability (MRI) or gravitational instability, depending upon a disc properties. While a PPD inner region is subject to MRI as the main source of the turbulence, the outer part of a massive enough PPD is gravitationally unstable. Although describing turbulence in terms of an effective viscosity is a very simplified approach due to non-linear and chaotic nature of this complex phenomenon, in the standard thin disc model all these complexities are baypassed when the azimuthal-radial component of the stress tensor is assumed to be proportional to the pressure.

The second key quantity is the rate of angular momentum injection by the binary, i.e., Λ. Although the angular momentum injection is restricted to a narrow anulus at the inner region of a disc and the function rapidly decreases with the distance, the injected angular momentum at the disc inner edge is able [to] affect global structure of a disc. [This tidal torque from the binary is defined as (Armitage & Natarajan 2002)] [

$$\Lambda(r) = {\rm sgn}(r-a_b)\frac{fq^2GM_c}{2r}\left(\frac{a_b}{\Delta_{\rm p}}\right)^4, \quad (2)$$

] [where f is a dimensionless normalization factor and $\Delta_{\rm p}$ is defined by $\Delta_{\rm p} = \max(H, r-a_b)$. Here, H is the disk scale height.]

The third key quantity is the wind mass-loss rate, i.e., $\dot{\Sigma}_{\rm w}$. Its mechanism is commonly attributed to the magnetically or photoevaporative mechanisms. [The significant radiation fields can lead to losing mass due to photoevaporation. Hence, the surface density profile decreases more rapidly with time. We use the model of Adams et al. (2004) and of AAN2013 to examine FUV evaporation due to external stars. So, we have] [

$$\dot{\Sigma}_{\rm w} = \frac{A}{4\pi}\left(\frac{r_g}{r}\right)^{\frac{3}{2}}\left[1+\frac{r_g}{r}\right]\exp\left(-\frac{r_g}{2r}\right), \quad (3)$$

] [where $A = Cn_{\rm d}c_s\mu$, and the constant C is of order unity. μ is the mean particle mass and is assumed to be $2.1m_H$. Here, r_g is a critical radius where the sound speed is comparable to the escape velocity. In fact, photoevaporation causes mass to become unbound near (and

outside) r_g. This radius is defined as] [

$$r_g = \frac{GM_c}{c_s^2} \approx 226\mathrm{AU}(\frac{M_c}{M_\odot})(\frac{T}{1000})^{-1}. \quad (4)$$

]

Comparisons of disc evolution with single and binary stars in the presence of external photoevaporation are then presented.

3. ANALYSIS

We solve surface density evolution equation (1) subject to boundary conditions ? and ? introduced by ?. An implicit finite difference method is adopted .... The initial disk mass is fixed at $M_{\rm d0} = 0.1$ M$_\odot$ and the initial surface density distribution is given by an exponentially truncated profile (e.g., Lynden-Bell & Pringle 1974)

[

$$\Sigma(r,0) = \frac{M_{\rm d0}}{2\pi(\exp(-\frac{r_{\rm in}}{r_{\rm d0}}) - e^{-1})r_{\rm d0}r} \exp(-r/r_{\rm d0}),\ r > 5a_{\rm b}. \quad (5)$$

]

$$\Sigma(r,0) = \frac{M_{\rm d0}}{2\pi(1-e^{-1})r_{\rm d0}r} \exp(r/r_{\rm d0}). \quad (6)$$

where $M_{\rm d0}$ and $r_{\rm d0}$ are the initial disk mass and radius. AAN2013 used standard boundary conditions (BCs), where the surface density tends to be zero at the inner edge $r_{\rm in}$ and the disk can expand freely at the outer radius. A large outer boundary for our computation domain is adopted, i.e.$r_{\rm out} = 20000$ AU.

[At the inner edge, we have a zero surface density inner boundary condition, but because the binary torque is strong, there is no material here. At the outer edge, we take a zero radial velocity boundary condition to prevent mass loss, but we have chosen a radius large enough that no significant amount of material spreads this far in a reasonable timescale. So, we can write] [

$$\Sigma(r,t)_{\rm r_{in}} = 0, \frac{\partial F_J}{\partial l}|_{\rm r_{out}} = 0, \quad (7)$$

]

In VGR2015, however, the following BCs are implemented:

$$\frac{\partial F_J}{\partial l}|_{\rm r_{in}} = \frac{F_J(r_{\rm in})}{l_{\rm in}}, \frac{\partial F_J}{\partial l}|_{\rm r_{out}} = 0, \quad (8)$$

where F_J is the viscous angular momentum flux defined as $F_J = 3\pi\nu\Sigma l$ and l is the specific angular momentum. In a circumstellar disk profile of F_J rapidly converge to $r^{1/2}$, whereas in a circumbinary disk F_J behavior tends to a flat distribution due to exerted binary torque at the inner edge. This interesting feature, however, is derived in the absence of winds. We can ran simulations with BCs used by AAN2013 or VGR2015, however, we prefer to implement those BCs introduced by VGR2015 with a mechanism of mass depletion. our goal is to explore circumbinary disk evolution with winds. Since VGR2015 studied circumbinary disc evolution subject to

To illustrate differences in a circumstellar disc evolution due to imposing the above BCs, we first perform evolution calculation for circumstellar disks using standard BCs used by AAN2015 and VGR2015.

Before presenting our results, it is more convenient to insure that our simulations are accurate in obtaining previous studies. To that purpose, we have recovered VGR2015 results for the circumbinary discs and findings of AAN2013 for a circumstellar disc orbiting a single star.

Our imposed boundary conditions, however, are different from those used by AAN2013 for a circumstellar disc. Figure 1 displays a circumstellar disc quantities corresponding to the BCs used by AAN2013 (dashed curves) and V (solid curves). The host star mass is fixed at $M = 1$ M$_\odot$ and the initial disc mass is $M_{\rm d} = 0.1$ M$_\odot$. Other model parameters are $\alpha = 0.01$

Material depleting by photoevaporative winds, however, occurs primarily at large radial distance and it gradually migrates to the inner region. A sharp outer disk edge, therefore, is created when a disk is exposed to external FUV radiation (AAN2013). There is a similar feature in the case of circumbinary disk illuminated by internal radiation field Alexander (2012). We, therefore, can provide quantitative estimates a circumbinary disk size irradiated by external FUV radiation field. To that purpose, the outer disk edge $r_{\rm d}$ is defined as radius where the enclosed mass is a fraction, say 0.99, of the total disk mass.

Figure 2 depicts surface density distribution (left) and the corresponding F_J profile for a circumbinary disk with photoevaporative wind due to external FUV radiation (solid curve) and without wind (dashed curve). Different colors correspond to different epochs, as labeled. The total mass of the primary and secondary stars with mass ratio $q = 1$ is $M = 1$ M$_\odot$. The binary separation is assumed to be $a_{\rm b} = 0.2$ AU and, thereby, the inner edge becomes $r_{\rm in} \simeq 2a_{\rm b} = 0.4$ AU. Other model parameters are $\alpha = 0.01$, ... Reduction of the surface density with time is due to the viscous stresses, however, this reduction is more pronounced when externally photoevaporative wind is included. Disk spreading in the absence of the wind is pronounced, however, photoevaporative winds strongly deplete outer regions and create a sharp outer edge.

A disk lifetime is set by the time that it losses 99 percent of its initial mass.

[Role of the viscosity parameter α on a circumbinary disk evolution ...] [Role of the viscosity parameter α is a circumbinary disk evolution is explored in Figure 4 by considering different values of this parameter, as labeled.

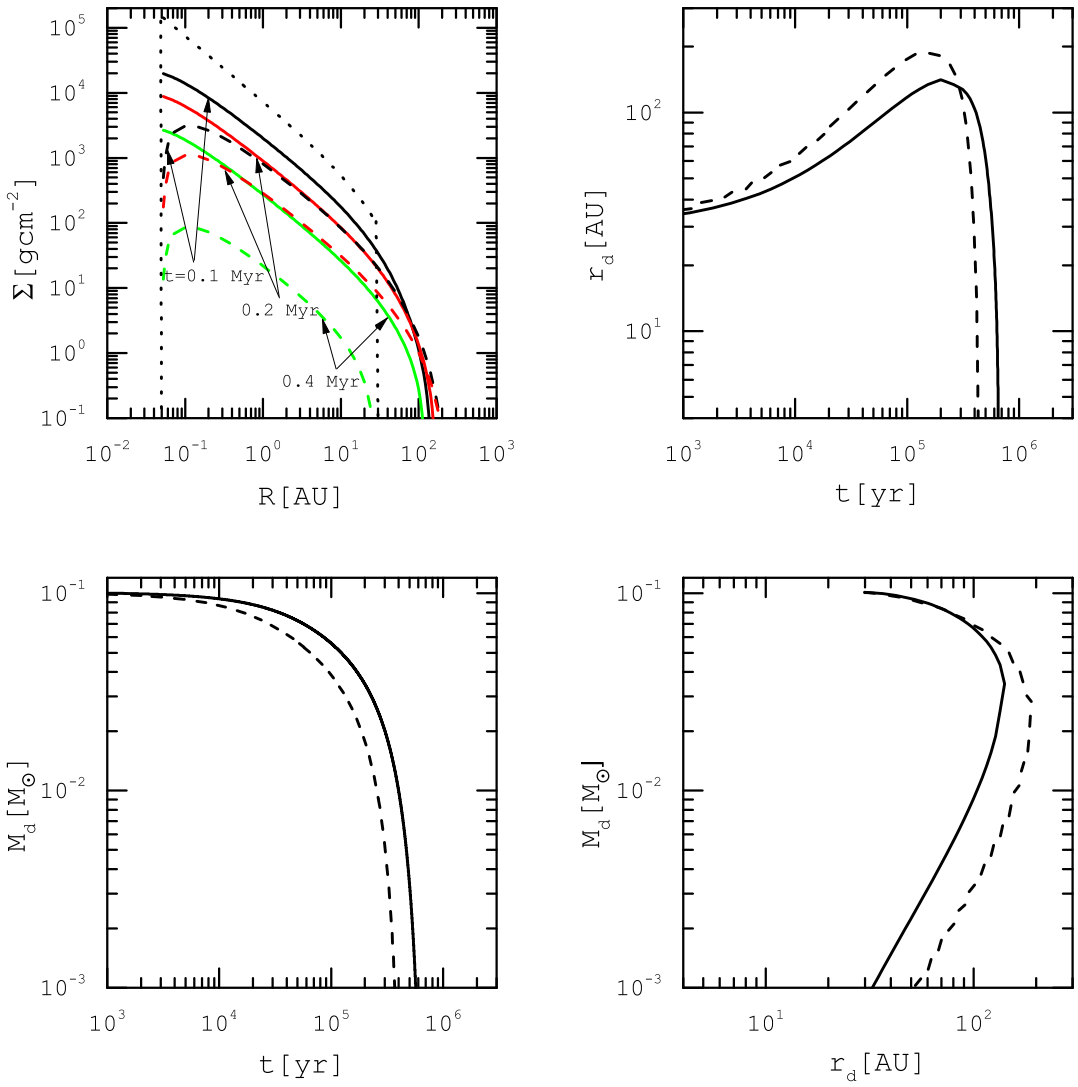

Figure 1. On the top left-hand panel, surface density profile of a disc orbiting a single star with mass $M_\star = 1$ M$_\odot$ is shown for different times, as labeled. Solid and dashed curves are corresponding to the solutions with BCs of AAN2015 and VGR2015 respectively. The initial surface density distribution is shown by a dotted curve. The adopted input parameters are $\alpha = 0.01$, $r_{\rm in} = 0.05$ AU ... . On the top right-hand panel, disk radius as a function of time is shown. On the bottom row, profiles of the disk mass (left) and evolutionary track in the plane of disk mass and radius (right) are shown for the presented solutions.

Other model parameters are $a_{\rm b} = 0.2AU$, $q = 1$ and $f = 1$. On the top panel, disk mass as a function of time is shown. We find that disk lifetime strongly depends on the adopted viscosity coefficient. A disk can survive over a longer time period if a lower viscosity coefficient is considered. A key feature of the viscous disk evolution is its extension to the larger radii due to the angular momentum transport. A higher viscosity coefficient, therefore, implies that disk material transport to the large radii to occur faster. Photoevaporative winds on the other hand are more efficient at a disk outer region. In a disk with a large viscosity coefficient, since the gas reaches to the outer part over a shorter time period,]

REFERENCES

Adams, F. C., Hollenbach, D., Laughlin, G., & Gorti, U. 2004, ApJ, 611, 360
Alexander, R. 2012, ApJL, 757, L29
Alexander, R. D., Clarke, C. J., & Pringle, J. E. 2006, MNRAS, 369, 229
Anderson, K. R., Adams, F. C., & Calvet, N. 2013, ApJ, 774, 9
Armitage, P. J. 2011, ARA&A, 49, 195
Armitage, P. J., & Natarajan, P. 2002, ApJL, 567, L9
Blandford, R. D., & Payne, D. G. 1982, MNRAS, 199, 883

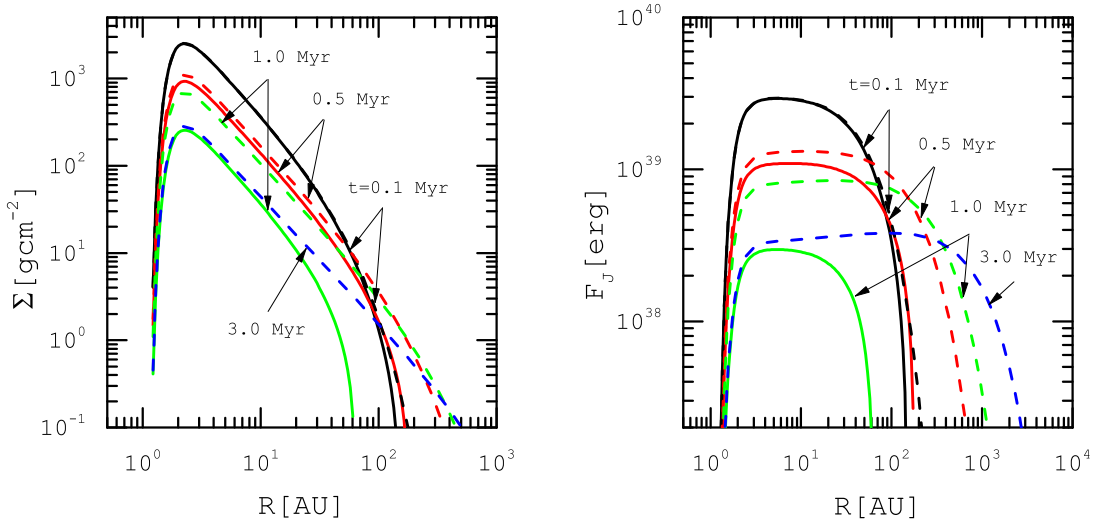

Figure 2. Profiles of the surface density (left) and the viscous angular momentum flux (right) for a circumbinary disk at different times, as lebeled. Masses of the primary and secondary stars are $M_{\rm p} = M_{\rm s} = 0.5$ M$_\odot$ and their separation is taken to be $a_{\rm b} = 0.2$ AU. [In this figure, we have $f = 1$ and $\alpha = 0.01$] Input parameters ? ... The circumbinary disk evolution with winds are displayed by solid curves, whereas solutions without winds are shown by dashed curves.

Doyle, L. R., et al. 2011, Science, 333, 1602
Ercolano, B., & Pascucci, I. 2017, Royal Society Open Science, 4, 170114
Gorti, U., Dullemond, C. P., & Hollenbach, D. 2009, ApJ, 705, 1237
Li, M., & Xiao, L. 2016, ApJ, 820, 36
Lynden-Bell, D., & Pringle, J. E. 1974, MNRAS, 168, 603
Martin, R. G., Armitage, P. J., & Alexander, R. D. 2013, ApJ, 773, 74
Orosz, J. A., et al. 2012, Science, 337, 1511
Owen, J. E., Ercolano, B., & Clarke, C. J. 2011, MNRAS, 412, 13
Owen, J. E., Ercolano, B., Clarke, C. J., & Alexander, R. D. 2010, MNRAS, 401, 1415
Rosotti, G. P., & Clarke, C. J. 2018, MNRAS, 473, 5630
Schwamb, M. E., et al. 2013, ApJ, 768, 127
Shakura, N. I., & Sunyaev, R. A. 1973, A&A, 24, 337
Vartanyan, D., Garmilla, J. A., & Rafikov, R. R. 2016, ApJ, 816, 94
Xiao, L., & Chang, Q. 2018, ApJ, 853, 22

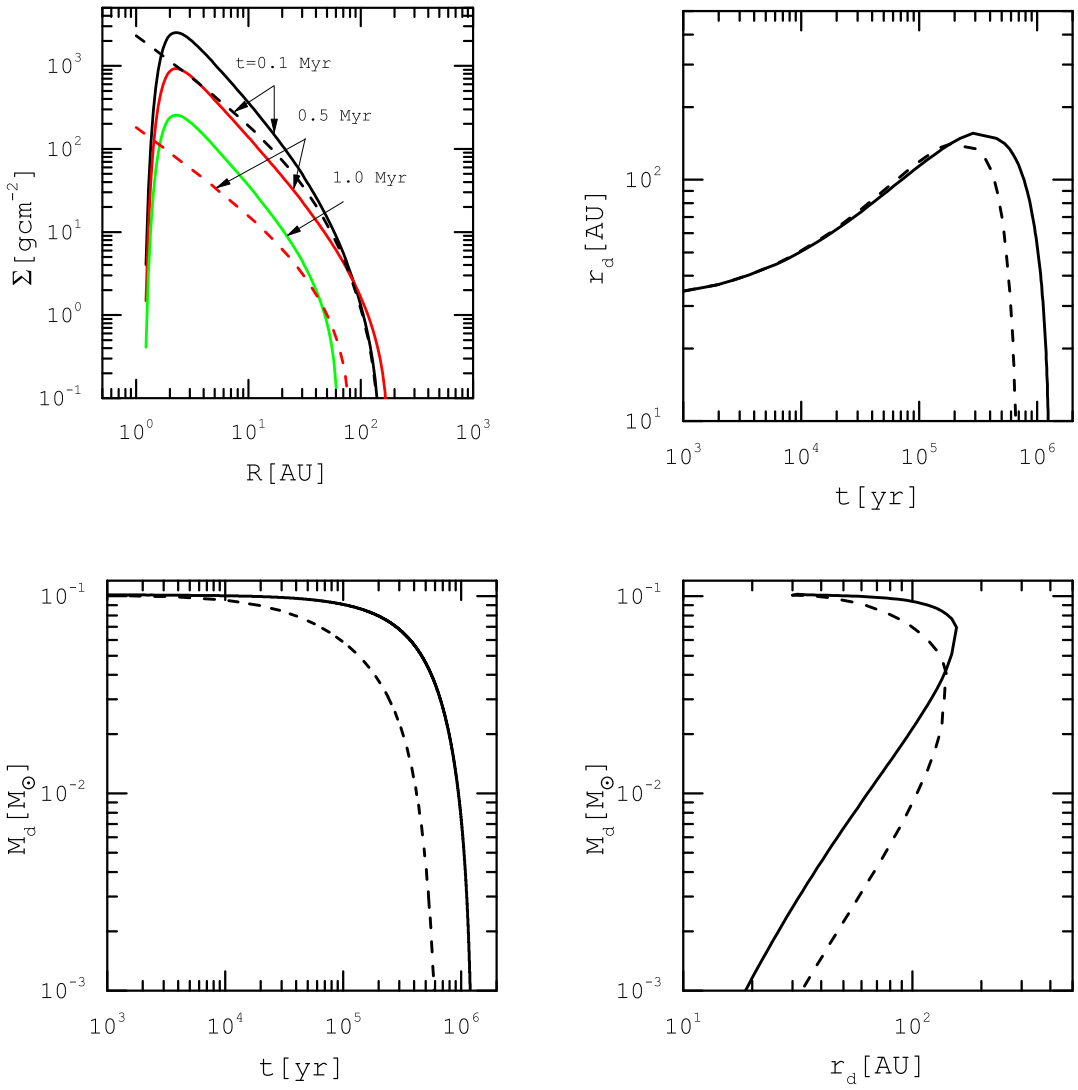

Figure 3. Physical quantities of a circumbinray disk (solid curves) and an identical single-star disk (dashed curves). Total mass of the binary is $M = 1$ M$\odot$ and separation of its components is assumed to be $a_{\rm b} = 0.2$ AU. Other model parameters are [$q = 1.0$, $\alpha = 0.01$, and $f = 1.0$.] On the top left-hand panel, surface density distribution is shown at different ephocs, as labeled. On the top right-hand panel, disk radius is shown through time. On the bottom left-hand panel, disk mass as a function of time is shown. On the bottom right-hand panel, the locus of points in the plane of disk mass and radius corresponding to the explored cases are shown.

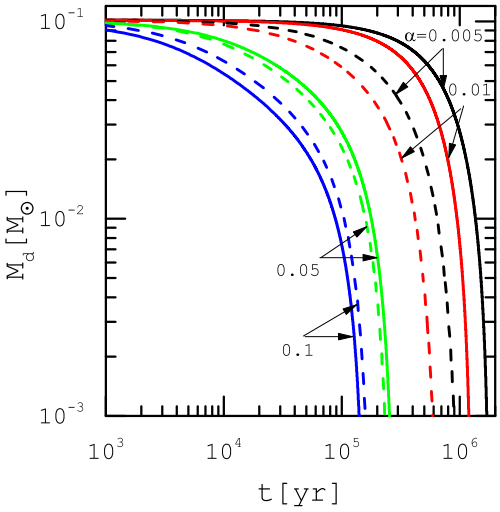

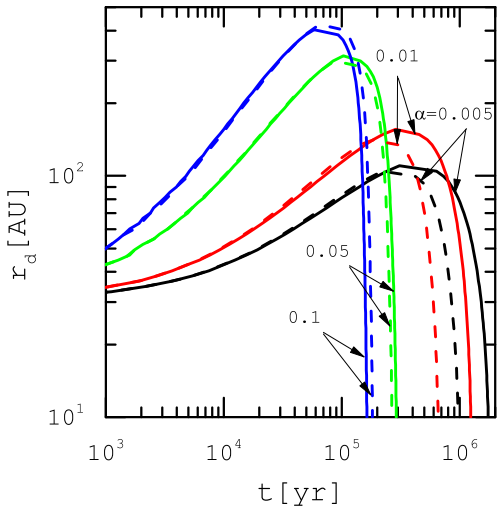

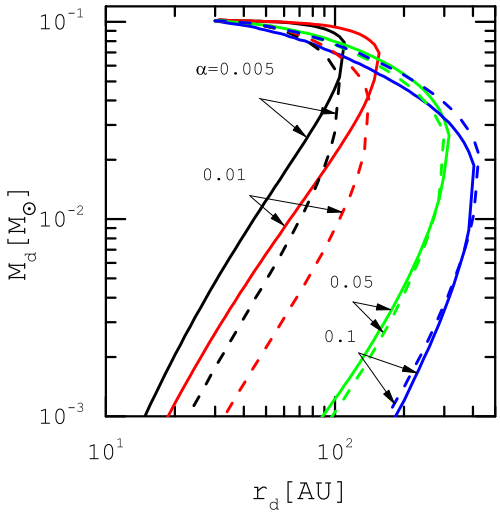

Figure 4. [Evolution of a circumbinary disk mass (top), its radius (middle) and the corresponding track in the disk mass and radius plane (bottom) are shown for different values of the viscosity parameter, as labeled. The input parameters are $a_{\rm b} = 0.2AU$, $q = 1$ and $f = 1$.]

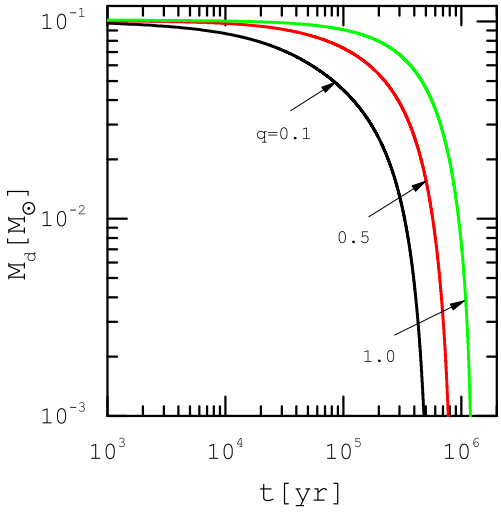

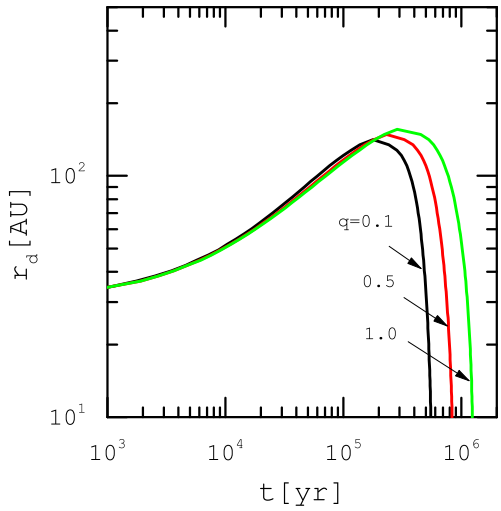

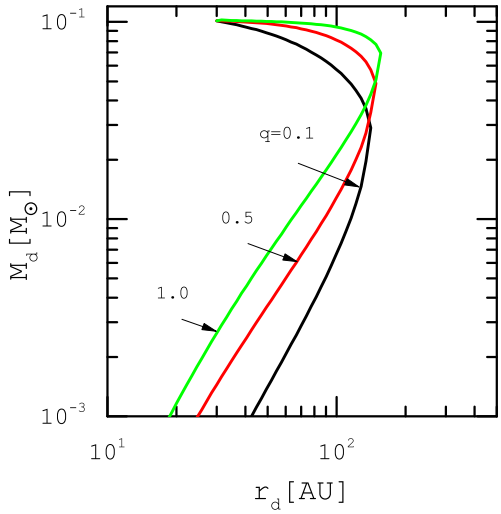

Figure 5. [Similar to Figure 4, but for different values of the binary mass ratio, as labeled. The input parameters are $a_{\rm b} = 0.2AU$, $\alpha = 0.01$ and $f = 1$.]

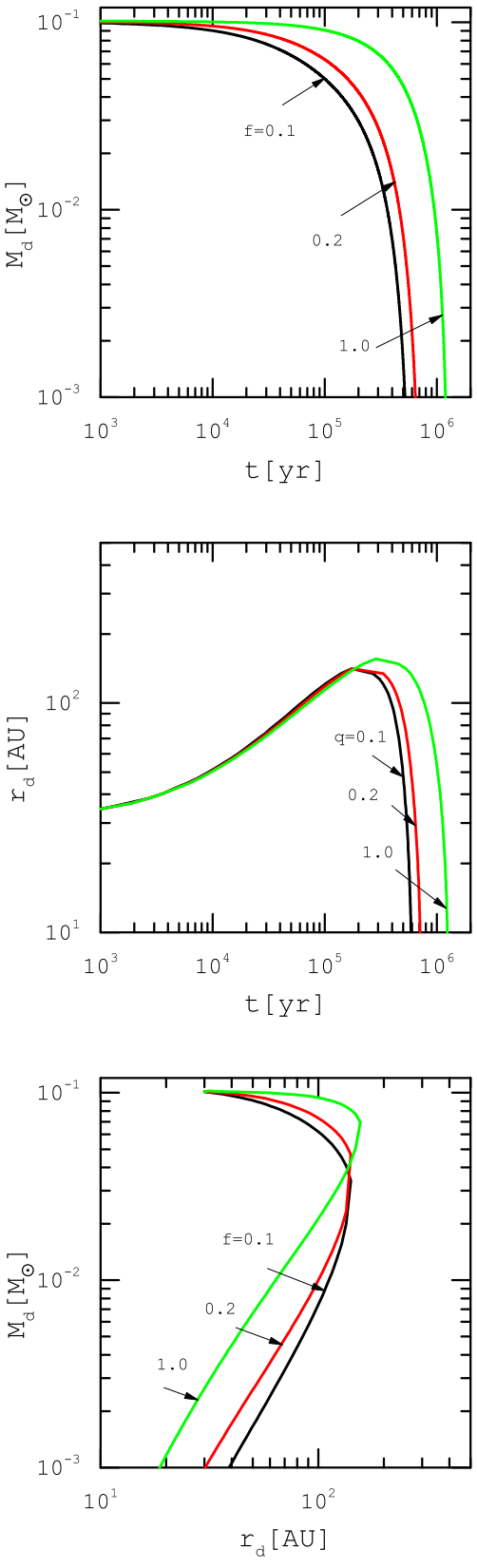

Figure 6. [Similar to Figure 4, but for different values of the binary torque coefficient, as labeled. The input parameters are $a_b = 0.2AU$, $\alpha = 0.01$ and $q = 1$.]

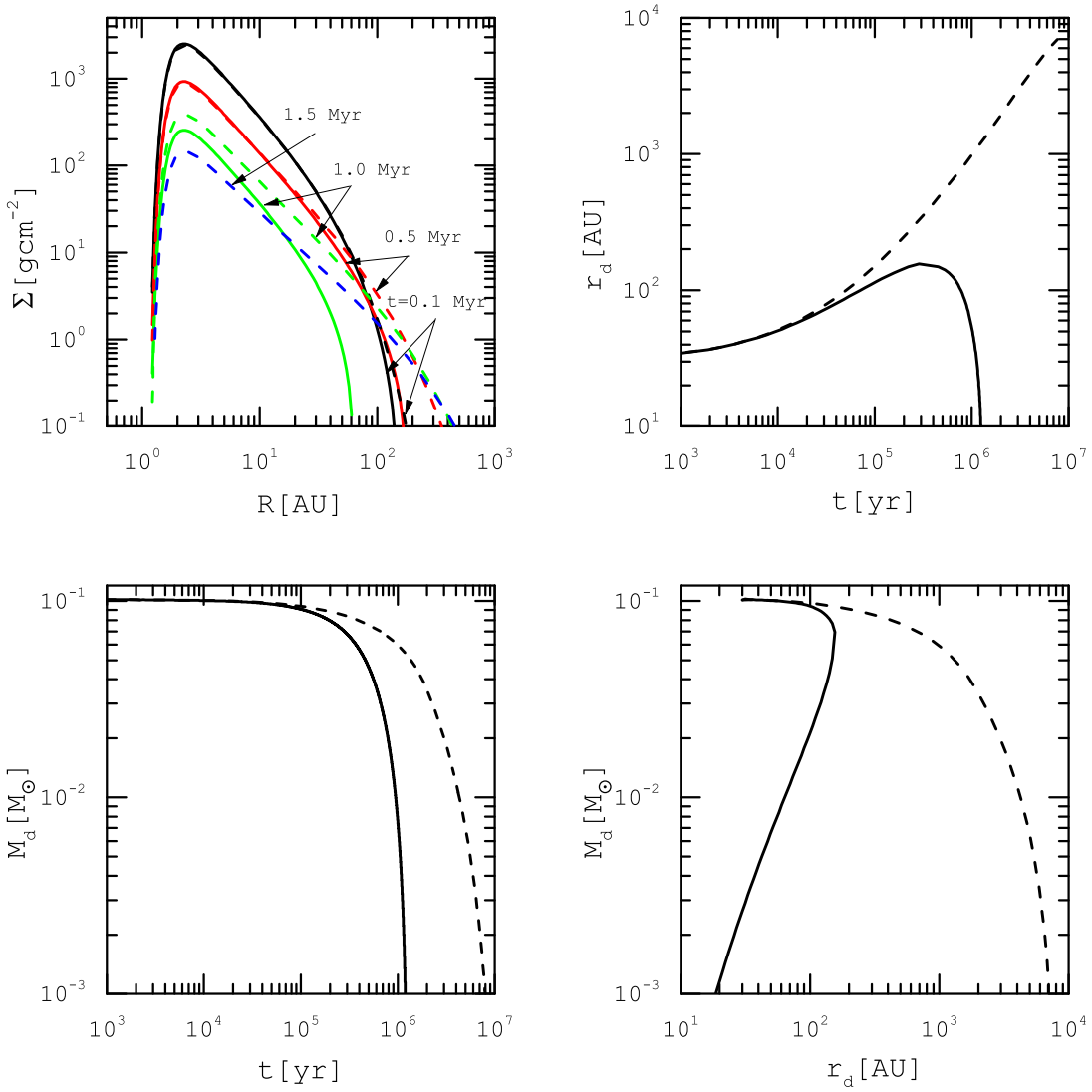

Figure 7. On the top left-hand panel, surface density profile of a disc orbiting a Binary star with mass $M_\star = 1$ $M_\odot$ is shown for different times, as labeled. Solid and dashed curves are corresponding to the cases with the external and the internal winds, respectively. The adopted input parameters are $\alpha = 0.01$, $q = f = 1.0$, and $a_{\rm b} = 0.2$AU. On the top right-hand panel, disk radius as a function of time is shown. On the bottom row, profiles of the disk mass (left) and evolutionary track in the plane of disk mass and radius (right) are shown for the presented solutions.